IAA-AAS-DyCoSS4-1-15

AAS 18-508

ORBIT RAISING AND DE-ORBIT FOR COPLANAR SATELLITE CONSTELLATIONS WITH LOW-THRUST PROPULSION

Simeng Huang,[*] Camilla Colombo,[†] and Franco Bernelli Zazzera[‡]

This paper deals with the planar transfer problem (i.e. orbit raising and de-orbiting phases) for low Earth orbit coplanar satellites constellation. The objectives are to minimize the total time of transfer and to maximize the miss distance during these phases so as to minimize the collision hazard. A Blended Error-Correction (BEC) steering law, consisting of tangential thrust and inertial thrust based on the offset in mean orbital parameters, is developed to design the transfer trajectory for a single satellite. The semi-analytical technique is used to evaluate the variation in orbital parameters over one orbit revolution to reduce the computation load. The numerical results show that the BEC steering law is able to identify near time-optimal solutions and the semi-analytical results have good accuracy. For multiple satellites transfer, the orbit transfer trajectory designed for a single satellite is used as a baseline for a global multi-satellite analysis of the miss distance among pair satellites during the orbit raising and de-orbiting phases. Considering limits on the transfer starting time for de-orbit mission, multi-objective optimization is used to find out the optimal transfer starting time for each satellite.

INTRODUCTION

In the recent past, several companies, including OneWeb, SpaceX and Samsung, disclosed their plan to build up large constellations consisting of hundreds to thousands of satellites in low Earth orbit (LEO). The purpose is to provide high-speed and global internet services, even to the most rural areas[1]. Latest news includes details about the setting up of assembly and test facilities for some of them, demonstrating that the large constellation is no more a notional proposal but will be a realistic space mission asset. With such a large number of satellites added to the LEO environment, a higher collision hazard will be posed to the operating objects in the already congested regime[2]. Therefore, the already operational demanding phases of orbit raising, from parking orbits up to the operational orbit, and de-orbit to re-entry altitudes are also challenged by a higher risk of collision. The electric low-thrust propulsion, which can provide continuous and high exhaust velocity so as to reduce the on-board fuel mass, will be used to execute the orbit transfer[3].

---

[*] PhD Student, Department of Aerospace Science and Technology, Politecnico di Milano, Via La Masa 34, 20156 Milano, Italy.

[†] Associate Professor, Department of Aerospace Science and Technology, Politecnico di Milano, Via La Masa 34, 20156 Milano, Italy.

[‡] Full Professor, Department of Aerospace Science and Technology, Politecnico di Milano, Via La Masa 34, 20156 Milano, Italy.

This paper deals with the orbit raising and de-orbiting phases, considering the requirements and constraints arising from the presence of multiple satellites. As a preliminary study, this paper focuses on planar transfer for coplanar satellites. The objectives of the mission design in this paper are to minimize the total time of transfer and to maximize the miss distance so as to lower the collision hazard as much as possible. The problem of orbit transfer for multiple satellites is conducted via two layers: the first layer is to design the time-optimal transfer trajectory for a single satellite; the second layer is to propose the transfer strategy for multiple satellites and to find out the optimal transfer starting time for each satellite by using multi-objective optimization.

Direct method has been widely used to solve the trajectory optimization problem with low-thrust propulsion. The idea is to transform the optimization problem into NonLinear Programming (NPL) problem by properly discretizing time. However, the number of design variables, which depends on the number of time nodes, is usually huge. Considering multiple satellites in this study, the direct method is not computationally efficient. Ruggiero et al. implemented a simple error-correction method for closed-loop guidance[4]. The idea is similar to feedback control and can also be used for designing steering law. Gao employed three simple steering laws, tangential steering, inertial steering and piecewise constant yaw steering over different orbital arcs in every revolution to efficiently change the semi-major axis, eccentricity and inclination, respectively[5]. Kluever et al. computed the time history of optimal thrust direction by blending the extremal feedback control laws, in this way he succeeded in changing the semi-major axis, eccentricity and inclination simultaneously[6]. To cope with the planar transfer problem for multiple satellites, this paper takes advantages of the References 4, 5, and 6 and develops a Blended Error-Correction (BEC) steering law, which is a blend of tangential thrust and inertial thrust based on the offset in mean orbital parameters.

Due to the low ratio of thrust-to-weight, the travel time might be up to several months and the transfer trajectory usually consists in hundreds to thousands of revolutions. The integration of such a long-duration trajectory is time-consuming. Therefore, semi-analytical technique is used in this paper to reduce the computation load.

The paper is organized as follows. Firstly, the dynamics model is presented. Then, the blended error-correction steering law is demonstrated after a brief introduction of the tangential thrust and the inertial thrust model; a numerical comparison is conducted to verify the feasibility of the proposed steering law. Next, two sets of semi-analytical solutions of orbital parameters (semi-major axis, eccentricity and argument of perigee) for both missions are derived; a numerical comparison is conducted to show the accuracy of these semi-analytical solutions. In the last section, the analysis for miss distance is firstly carried out, base on which, the transfer strategy for a given test case is proposed; considering the limits on transfer starting time for de-orbit mission, the technique of multi-objective optimization is used to find out the optimal transfer starting time for each satellite.

DYNAMICS MODEL

The scope of the present work is planar transfers. So the thrust acceleration vector lies within the orbital plane and the orbital parameters to be discussed are semi-major axis, eccentricity, argument of perigee and (true, eccentric and mean) anomaly.

The derivatives of orbital parameters given by Gauss' equations[7] in terms of thrust acceleration are

$$\frac{\mathrm{d}a}{\mathrm{d}t} = \frac{2a^2}{h}\left(e\sin\theta u_r + \frac{p}{r}u_\theta\right) \tag{1}$$

$$\frac{de}{dt} = \frac{1}{h}\left(p\sin\theta u_r + \left((p+r)\cos\theta + re\right)u_\theta\right) \qquad (2)$$

$$\frac{d\omega}{dt} = \frac{1}{he}\left(-p\cos\theta u_r + (p+r)\sin\theta u_\theta\right) \qquad (3)$$

$$\frac{dE}{dt} = \frac{na}{r} + \frac{1}{nae}\left((\cos\theta - e)u_r - \left(1+\frac{r}{a}\right)\sin\theta u_\theta\right) \qquad (4)$$

where, u_r and u_θ are the radial and transversal components of the thrust acceleration vector respectively, a is the semi-major axis, e is the eccentricity, ω is the argument of perigee, E is the eccentric anomaly, θ is the true anomaly, $r = a(1 - e\cos E)$ is the orbit radius, $p = a(1 - e^2)$ is the semi-latus rectum, $h = (\mu p)^{1/2}$ is the angular momentum with μ being the Earth's gravitational constant, $n = (\mu/a^3)^{1/2}$ is the mean motion. Because the thrust acceleration is much smaller (usually $\leq 10^{-6}$ km/s^2) than the gravitational acceleration ($> 10^{-4}$ km/s^2), the derivative of the eccentric anomaly can be approximated as

$$\frac{dE}{dt} \approx \frac{na}{r} \qquad (5)$$

The relation between true anomaly and eccentric anomaly is given by[8]

$$\sin\theta = \frac{\sin E\sqrt{1-e^2}}{1-e\cos E}, \quad \cos\theta = \frac{\cos E - e}{1-e\cos E} \qquad (6)$$

Then dividing Eqs. (1) – (3) by Eq. (5) and substituting Eq. (6), after some manipulations, the derivatives of orbital parameters with respect to eccentric anomaly are derived:

$$\frac{da}{dE} = \frac{2a^3}{\mu}\left(e\sin E u_r + \sqrt{1-e^2}u_\theta\right) \qquad (7)$$

$$\frac{de}{dE} = \frac{a^2}{\mu}\left((1-e^2)\sin E u_r + \sqrt{1-e^2}\left(2\cos E - e - e\cos^2 E\right)u_\theta\right) \qquad (8)$$

$$\frac{d\omega}{dE} = \frac{a^2}{\mu e}\left(\sqrt{1-e^2}\,(e-\cos E)u_r + \left(2-e^2 - e\cos E\right)\sin E u_\theta\right) \qquad (9)$$

Eqs. (7) – (9) will be integrated to evaluate the variations of orbital parameters over one revolution with the use of semi-analytic techniques, previous to which, the steering law should firstly be defined.

STEERING LAW

For low-thrust propulsion, the magnitude of thrust force is fixed by the thruster; only the thrust direction is controllable. The in-plane thrust direction is described by the pitch angle α, defined in this paper as the angle measured counterclockwise from the orbit radius direction to the thrust direction, shown in Figure 1.
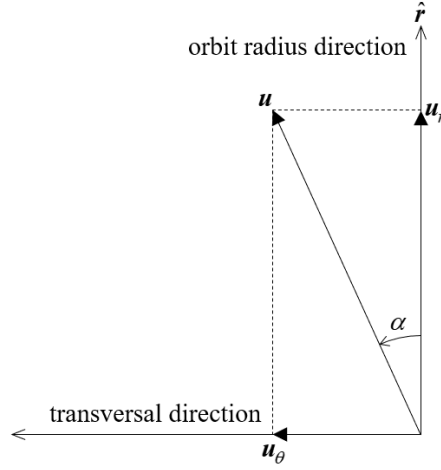
Figure 1 Definition of the pitch angle.

The radial and transversal components of the thrust acceleration vector are given by

$$u_r = u \cos \alpha \, , \; u_\theta = u \sin \alpha \tag{10}$$

where u is the magnitude of the thrust acceleration vector, given by[9]

$$u = \frac{2 \eta P}{m g_0 I_{sp}} \tag{11}$$

with η being the efficiency, P being the power, g_0 being the Earth's gravitational acceleration at sea-level, I_{sp} being the specific impulse, and m being the spacecraft mass. The loss of spacecraft mass is governed by[9]

$$\frac{\mathrm{d}m}{\mathrm{d}t} = -m \frac{u}{g_0 I_{sp}} \tag{12}$$

One objective of this paper is to minimize the total time of transfer for multiple satellites. Therefore for a single satellite, the transfer trajectory needs to be designed to be time-optimal. Two steering laws, tangential thrust and inertial thrust, are used and blended to simultaneously change semi-major axis and eccentricity. Apart from the advantage of time efficiency, these two steering laws also benefit the integration for the single-average technique, because the derivatives of the orbital parameters by these two steering laws can be expressed in a simple fashion.

Tangential Thrust

The tangential thrust is the most efficient steering law to change the semi-major axis, an instantaneously optimal solution is derived by setting $\partial(\mathrm{d}a/\mathrm{d}E)/\partial\alpha = 0$. The thrust vector is always aligned with the velocity vector. If the pitch angle is set to be equal to the flight path angle γ (the angle between radius vector and velocity vector), i.e., $\alpha = \gamma$, then the thrust direction is along the velocity direction and the semi-major axis will be instantaneously increased. If the pitch angle is set as $\alpha = \gamma + \pi$, then the thrust direction is opposite to the velocity direction and the semi-major axis will be instantaneously decreased.

According to the relation between flight path angle and eccentric anomaly, which is

$$\sin\gamma = \frac{\sqrt{1-e^2}}{\sqrt{1-e^2\cos^2 E}} \ , \quad \cos\gamma = \frac{e\sin E}{\sqrt{1-e^2\cos^2 E}} \tag{13}$$

u_r and u_θ are given by

$$u_r = \pm\frac{e\sin E}{\sqrt{1-e^2\cos^2 E}}u \ , \quad u_\theta = \pm\frac{\sqrt{1-e^2}}{\sqrt{1-e^2\cos^2 E}}u \tag{14}$$

where the sign + and – represent that the semi-major axis is to be increased and decreased respectively.

Substituting Eq. (14) into Eqs. (7) – (9), the derivatives of the orbital parameters with respect to the eccentric anomaly by using tangential thrust are derived:

$$\left(\frac{da}{dE}\right)_t = \pm\frac{2a^3}{\mu}u\sqrt{1-e^2\cos^2 E} \tag{15}$$

$$\left(\frac{de}{dE}\right)_t = \pm\frac{2a^2\left(1-e^2\right)}{\mu}u\sqrt{\frac{1-e\cos E}{1+e\cos E}}\cos E \tag{16}$$

$$\left(\frac{d\omega}{dE}\right)_t = \pm\frac{2a^2\sqrt{1-e^2}}{\mu e}u\sqrt{\frac{1-e\cos E}{1+e\cos E}}\sin E \tag{17}$$

Inertial Thrust

The inertial thrust is a near optimal steering law to change the eccentricity[5,10]. The thrust vector is always perpendicular to the periapsis. If the pitch angle is set to $\alpha = \pi/2 - \theta$, then the eccentricity will be increased. If the pitch angle is set to $\alpha = 3\pi/2 - \theta$, then the eccentricity will be decreased.

According to Eq. (6), which is the relation between true anomaly and eccentric anomaly, u_r and u_θ are given by[8]

$$u_r = \pm\frac{\sin E\sqrt{1-e^2}}{1-e\cos E}u \ , \quad u_\theta = \pm\frac{\cos E-e}{1-e\cos E}u \tag{18}$$

where the sign + and – represent that the eccentricity is to be increased and decreased respectively.

Substituting Eq. (14) into Eqs. (7) – (9), the derivatives of orbital parameters with respect to eccentric anomaly by inertial thrust are derived:

$$\left(\frac{da}{dE}\right)_i = \pm\frac{2a^3\sqrt{1-e^2}}{\mu}u\cos E \tag{19}$$

$$\left(\frac{de}{dE}\right)_i = \pm\frac{a^2\sqrt{1-e^2}}{\mu}u\left(\cos^2 E - 2e\cos E + 1\right) \tag{20}$$

$$\left(\frac{d\omega}{dE}\right)_i = \pm\frac{a^2}{\mu e}u\left(\cos E - e\right)\sin E \tag{21}$$

Blended Error-Correction (BEC) Steering Law

The final thrust acceleration is obtained by blending the tangential and inertial thrust based on the offset in the orbital parameters, expressed as follows:

$$\boldsymbol{u} = c_t \boldsymbol{u}_t + c_i \boldsymbol{u}_i \tag{22}$$

where, $\boldsymbol{u}_t$ and $\boldsymbol{u}_i$ are the tangential and inertial thrust acceleration vector respectively, c_t and c_i are the coefficients for the tangential and inertial thrust, respectively.

The error in the orbital parameter is defined as the ratio between the error of the instantaneous mean orbital parameter with respect to the target value and the difference between the initial value and the target value[4]. The errors in semi-major axis and eccentricity are given by

$$k_a = \frac{a_f - a}{\left| a_f - a_0 \right|} \;, \quad k_e = \frac{e_f - e}{\left| e_f - e_0 \right|} \tag{23}$$

where, a_f and e_f are the desired target values of semi-major axis and eccentricity, whereas a_0 and e_0 are the initial values, the symbol $|\square|$ represents the absolute value of the generic variable $\square$.

As abovementioned, the orbital parameters which are mostly changed by tangential and inertial thrust are the semi-major axis and the eccentricity respectively. Therefore, c_t and c_i are set to be proportional to k_a and k_e, respectively. Noticing that the magnitudes of $\boldsymbol{u}_t$ and $\boldsymbol{u}_i$ are u, c_t and c_i must be normalized. After using the cosine law, c_t and c_i are given by

$$c_t = \frac{k_a}{\sqrt{k_a^2 + k_e^2 + 2 k_a k_e \cos\langle \boldsymbol{u}_t, \boldsymbol{u}_i \rangle}} \;, \quad c_i = \frac{k_e}{\sqrt{k_a^2 + k_e^2 + 2 k_a k_e \cos\langle \boldsymbol{u}_t, \boldsymbol{u}_i \rangle}} \tag{24}$$

where $\langle \boldsymbol{u}_t, \boldsymbol{u}_i \rangle$ represents the angle between $\boldsymbol{u}_t$ and $\boldsymbol{u}_i$, and $\cos\langle \boldsymbol{u}_t, \boldsymbol{u}_i \rangle$ is given by

$$
\begin{aligned}
\cos\langle \boldsymbol{u}_t, \boldsymbol{u}_i \rangle &= \mathrm{sign}(k_a)\,\mathrm{sign}(k_e)\sin(\gamma + \theta) \\
&= \mathrm{sign}(k_a)\,\mathrm{sign}(k_e)\left(\frac{\sqrt{1-e^2}\,(\cos E - e)}{(1 - e\cos E)\sqrt{1 - e^2 \cos^2 E}} + \frac{e\sin^2 E}{\sqrt{1 + e\cos E}} \right)
\end{aligned}
\tag{25}
$$

with sign $(\square)$ being the sign of the generic variable $\square$.

With the use of the BEC steering law, the derivatives of the orbital parameters with respect to the eccentric anomaly are given in the following form:

$$\frac{\mathrm{d}\boldsymbol{x}}{\mathrm{d}E} = c_t \left(+\frac{\mathrm{d}\boldsymbol{x}}{\mathrm{d}E} \right)_t + c_i \left(+\frac{\mathrm{d}\boldsymbol{x}}{\mathrm{d}E} \right)_i \tag{26}$$

where, $\boldsymbol{x} = [a, e, \omega]^T$, $(+\mathrm{d}\boldsymbol{x}/\mathrm{d}E)_t$ and $(+\mathrm{d}\boldsymbol{x}/\mathrm{d}E)_i$ are given by Eqs. (15) – (17) and Eqs. (19) – (21) respectively with the sign $+$ representing that the signs of the equations are positive.

Numerical Results

To verify the feasibility of the devised models, a comparison is conducted between the trajectories obtained by the BEC and the optimal steering law for a de-orbit mission. Here, the optimal steering law

$$u_r = \frac{(1-e)^2 \sin E}{\sqrt{(1-e)^4 \sin^2 E + (1-e^2)\left(4\sin^2\frac{E}{2} - e\sin^2 E\right)^2}} u$$

$$u_\theta = -\frac{\sqrt{1-e^2}\left(4\sin^2\frac{E}{2} - e\sin^2 E\right)}{\sqrt{(1-e)^4 \sin^2 E + (1-e^2)\left(4\sin^2\frac{E}{2} - e\sin^2 E\right)^2}} u$$

(27)

is derived by setting $\partial a(1-e)/\partial E = 0$ and $\partial^2 a(1-e)/\partial E^2 \geq 0$ such that the perigee can be lowered fastest. The reason why not using this optimal steering law for de-orbit mission is because, for this complicated form it is difficult to obtain the semi-analytic solutions; this will be attempted in a future extension of this work.

Table 1 lists the characteristics of the spacecraft considered. The data is from PARASOL, a small LEO satellite[11]. Table 2 lists the initial and the stopping conditions for the test case of de-orbit mission, where $h_f = a(1-e) - R_E$ is the target re-entry altitude of the perigee. Note that the initial eccentricity is set to be 10^{-4} instead of 0 to accommodate with the singularity in the derivative of argument of perigee in Eq. (3).

Table 1 Characteristics of the spacecraft

m_0 (kg)	Thruster	η (%)	P (W)	I_{sp} (s)
120	Stationary Plasma Thruster (SPT)	39.23	150	1500

Table 2 Parameters for the de-orbit mission

| Initial condition				Stopping condition
a_0 (km)	e_0	ω_0 (deg)	E_0 (deg)	h_f (km)
$1200 + R_E$	10^{-4}	0	0	300

The target values in Eq. (23) is set to $a_f = (300 + R_E)$ and $e_f = 1$, respectively. Figure 2 to Figure 4 present the comparison between the optimal and the BEC steering law in terms of perigee altitude, semi-major axis and eccentricity. The travel time of the optimal and BEC method are 73.52 days and 76.63 days respectively. The error of the travel time, defined by the ratio of the difference between the travel time obtained by the two steering laws and the travel time obtained by the optimal steering law, is relatively small, equal to 4.29%. This is enough to demonstrate that the BEC method is near time-optimal. From the comparison of semi-major axis and eccentricity, it can be seen that the time history of the perigee altitude by the BEC method is very close to the optimal method even if there are obvious differences in semi-major axis and eccentricity.
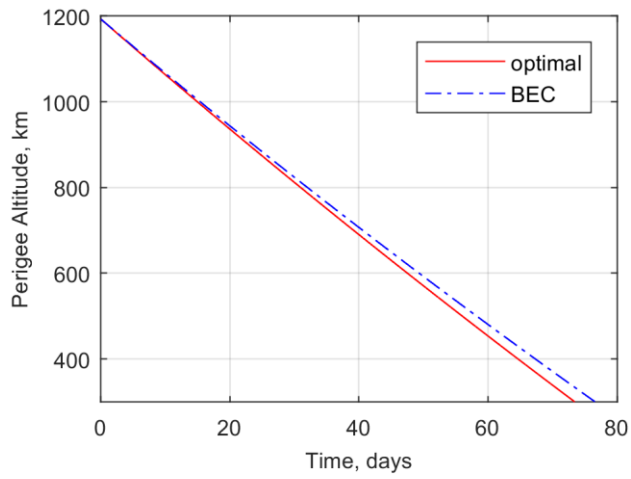
Figure 2 Comparison in the perigee altitude.
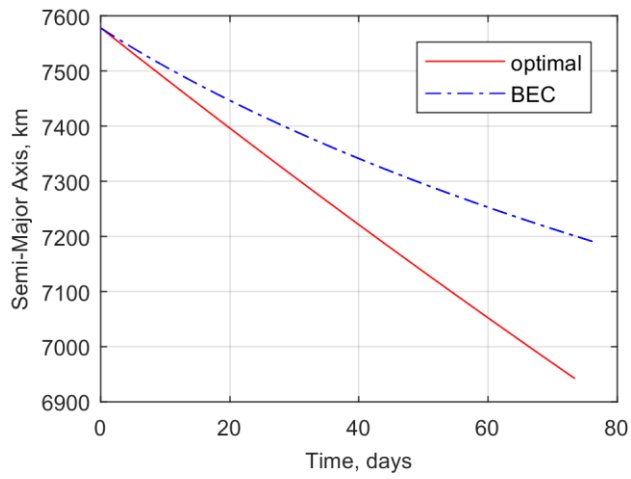
Figure 3 Comparison in the semi-major axis.
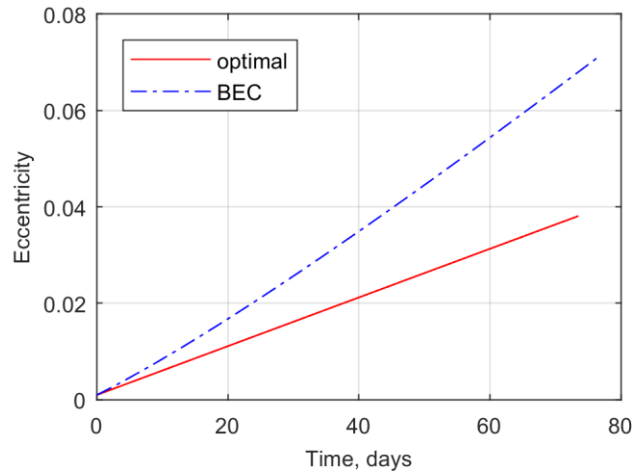
Figure 4 Comparison in the eccentricity.

SEMI-ANALYTICAL TECHNIQUE

The magnitude of the low-thrust acceleration is typically on the order of $10^{-4}g$ or less[12]. In a single orbit revolution, the variation in a, e and ω due to such a small force is negligible and it is enough to assume a, e and ω to be constant over one orbit revolution. Then the transfer trajectory is obtained by updating the orbital parameters after every revolution until the stopping condition is reached. The integration problem is transformed into evaluating the variations of orbital parameters over one revolution:

$$\int_0^{2\pi} \frac{d\boldsymbol{x}}{dE}\,dE = \int_0^{2\pi}\left(c_t\left(+\frac{d\boldsymbol{x}}{dE}\right)_t + c_i\left(+\frac{d\boldsymbol{x}}{dE}\right)_i \right)dE \tag{28}$$

Note that the lower and upper limit of the integral should be the entrance and exit eccentric anomaly in eclipse. However as a preliminary study, the Earth's shadow effect will not be considered in this paper, neither will the J_2 effect. This will be done in a future work.

No closed-form solution exists for Eq. (28). It is thus necessary to expand them in power of eccentricity, which is small (≤ 0.1) for LEO missions, before integrating. Thanks to the simple form of Eqs. (15) – (17) and Eqs. (19) – (21), the only term to be expanded is the denominator of the coefficients, i.e., $\left(k_a^2 + k_e^2 + 2k_a k_e \cos\langle \boldsymbol{u}_t, \boldsymbol{u}_i \rangle\right)^{-1/2}$.

Orbit Raising

The orbit raising mission in this paper is assumed to raise the spacecraft from the near-circular parking orbit to the circular operating orbit. The errors in semi-major axis and eccentricity are given accordingly to

$$k_a^r = \frac{\Delta a}{a_f - a_0}, \quad k_e^r = -\frac{e}{e_0} \tag{29}$$

where, the superscript r represents the mission of orbit raising, and $\Delta a = a_f - a$.

Then substituting Eq. (29) into Eq. (24) and expanding the term $\left(k_a^2 + k_e^2 + 2k_a k_e \cos\langle \boldsymbol{u}_t, \boldsymbol{u}_i \rangle\right)^{-1/2}$ up to $O(e^2)$, the coefficients of the tangential and inertial thrust can be approximated as

$$c_t^r \approx R, \quad c_i^r \approx -\frac{a_f - a_0}{e_0}\frac{e}{\Delta a}R \tag{30}$$

where R is a polynomial in the eccentricity, given by

$$R = 1 + \frac{a_f - a_0}{e_0 \Delta a}\cos E\, e + \frac{(a_f - a_0)^2}{e_0^2 \Delta a^2}\frac{3\cos^2 E - 1}{2}e^2 \tag{31}$$

Substituting Eq. (30) into Eq. (26), after some manipulations, the variations of orbital parameters over one revolution for orbit raising are derived:

103

$$\Delta a^r = \int_0^{2\pi} \left(c_t^r \left(+\frac{\mathrm{d}a}{\mathrm{d}E} \right)_t + c_i^r \left(+\frac{\mathrm{d}a}{\mathrm{d}E} \right)_i \right) \mathrm{d}E$$

$$= \frac{4\pi a^3}{\mu} \left(1 + \frac{(1-2\sqrt{1-e^2})(a_f - a_0)^2 - e_0^2 \Delta a^2}{4e_0^2 \Delta a^2} e^2 \right) u \tag{32}$$

$$\Delta e^r = \int_0^{2\pi} \left(c_t^r \left(+\frac{\mathrm{d}e}{\mathrm{d}E} \right)_t + c_i^r \left(+\frac{\mathrm{d}e}{\mathrm{d}E} \right)_i \right) \mathrm{d}E$$

$$= \frac{2\pi a^2 \sqrt{1-e^2}}{\mu} \left(\left(\frac{(2\sqrt{1-e^2}-3)(a_f - a_0)}{2e_0 \Delta a} - \sqrt{1-e^2} \right) e - \frac{(a_f - a_0)^2 \left(9(a_f - a_0) - 16e_0 \Delta a \right)}{16 e_0^3 \Delta a^3} e^3 \right) u \tag{33}$$

$$\Delta \omega^r = \int_0^{2\pi} \left(c_t^r \left(+\frac{\mathrm{d}\omega}{\mathrm{d}E} \right)_t + c_i^r \left(+\frac{\mathrm{d}\omega}{\mathrm{d}E} \right)_i \right) \mathrm{d}E = 0 \tag{34}$$

De-Orbiting

An efficient de-orbit strategy is to lower the perigee to the point where the atmospheric drag will lower the apogee quickly until the natural re-entry happens. To lower the perigee as fast as possible, the target semi-major axis and eccentricity are chosen as

$$a_f = h_f + R_\oplus$$
$$e_f = 1 \tag{35}$$

Then the errors of semi-major axis and eccentricity are

$$k_a^d = \frac{\Delta a}{a_0 - a_f}, \quad k_e^d = \Delta e \tag{36}$$

where, the superscript d represents the mission of de-orbiting, and $\Delta e = e_f - e$.

Similar to orbit raising, substituting Eq. (36) into Eq. (24) and expanding the term $\left(k_a^2 + k_e^2 + 2k_a k_e \cos\langle u_t, u_i \rangle \right)^{-1/2}$ up to $O(e^2)$, the coefficients of the tangential and inertial thrust can be approximated as

$$c_t^d = \Delta a D, \quad c_i^d = (a_0 - a_f)\Delta e D \tag{37}$$

where D is a polynomial in the eccentricity, given by

$$D = \frac{D_0}{\left((a_0 - a_f)^2 + \Delta a^2 + 2(a_0 - a_f)\Delta a \cos E \right)^{1/2}}$$
$$+ \frac{D_1}{\left((a_0 - a_f)^2 + \Delta a^2 + 2(a_0 - a_f)\Delta a \cos E \right)^{3/2}} e \tag{38}$$
$$+ \frac{D_2}{\left((a_0 - a_f)^2 + \Delta a^2 + 2(a_0 - a_f)\Delta a \cos E \right)^{5/2}} e^2$$

with D_0, D_1 and D_2 being

$$D_0 = 1$$

$$D_1 = (a_0 - a_f)\big((a_0 - a_f) + \Delta a \cos E\big) \tag{39}$$

$$D_2 = \frac{a_0 - a_f}{4}\left(\begin{array}{c} (a_0 - a_f)\big(4(a_0 - a_f)^2 + 3\Delta a^2\big) + 2\big(5(a_0 - a_f)^2 + \Delta a^2\big)\Delta a \cos E \\ +3(a_0 - a_f)\Delta a^2 \cos 2E - 2\big((a_0 - a_f)^2 + \Delta a^2\big)\Delta a \cos 3E - 2(a_0 - a_f)\Delta a^2 \cos 4E \end{array}\right)$$

Substituting Eq. (37) into Eq. (26), after some manipulations, the variations of orbital parameters over one revolution for de-orbit are derived:

$$\begin{aligned} \Delta a^d &= \int_0^{2\pi}\left(c_t^d\left(+\frac{\mathrm{d}a}{\mathrm{d}E}\right)_t + c_i^d\left(+\frac{\mathrm{d}a}{\mathrm{d}E}\right)_i \right)\mathrm{d}E \\ &= \frac{2a^3}{\mu}\left(\frac{1}{a_0 - a}\big(\Delta a d_F^{at} + \sqrt{1-e^2}\,\Delta e d_F^{ai}\big)elliF + (a_0 - a)\big(\Delta a d_E^{at} + \sqrt{1-e^2}\,\Delta e d_E^{ai}\big)elliE \right)u \end{aligned} \tag{40}$$

$$\begin{aligned} \Delta e^d &= \int_0^{2\pi}\left(c_t^d\left(+\frac{\mathrm{d}e}{\mathrm{d}E}\right)_t + c_i^d\left(+\frac{\mathrm{d}e}{\mathrm{d}E}\right)_i \right)\mathrm{d}E \\ &= \frac{a^2\sqrt{1-e^2}}{\mu}\left(\frac{1}{a_0 - a}\big(\sqrt{1-e^2}\,\Delta a d_F^{et} + (a_0 - a_f)\Delta e d_F^{ei}\big)elliF + (a_0 - a)\big(\sqrt{1-e^2}\,\Delta a d_E^{et} + (a_0 - a_f)\Delta e d_E^{ei}\big)elliE \right)u \end{aligned}$$

$$\tag{41}$$

$$\Delta\omega^d = \int_0^{2\pi}\left(c_t^d\left(+\frac{\mathrm{d}\omega}{\mathrm{d}E}\right)_t + c_i^d\left(+\frac{\mathrm{d}\omega}{\mathrm{d}E}\right)_i \right)\mathrm{d}E = 0 \tag{42}$$

where d_F^{at}, d_E^{at}, d_F^{ai}, d_E^{ai}, d_F^{et}, d_E^{et}, d_F^{ei} and d_E^{ei} are the binomials of eccentricity in the form of $d\# = d_0\# + d_1\#e + d_2\#e^2$, with the subscripts 0, 1 and 2 being the coefficients of e^0, e^1 and e^2 respectively, given by

$$\begin{aligned} d_{0F}^{at} &= 2 \\ d_{1F}^{at} &= 1 \\ d_{2F}^{at} &= -\frac{3(a_0 - a_f)^4 + 3(a_0 - a_f)^2 \Delta a^2 + 3\Delta a^4}{2(a_0 - a_f)^2 \Delta a^2} \end{aligned} \tag{43}$$

$$\begin{aligned} d_{0E}^{at} &= 0 \\ d_{1E}^{at} &= \frac{1}{(a_0 - a_f)^2 - \Delta a^2} \\ d_{2E}^{at} &= \frac{3(a_0 - a_f)^6 - 4(a_0 - a_f)^2 \Delta a^4 + 3\Delta a^6}{2(a_0 - a_f)^2 \Delta a^2 \big((a_0 - a_f)^2 - \Delta a^2\big)^2} \end{aligned} \tag{44}$$

$$d_{0F}^{ai} = -\frac{\left(a_0 - a_f\right)^2 + \Delta a^2}{\Delta a}$$

$$d_{1F}^{ai} = -\Delta a \tag{45}$$

$$d_{2F}^{ai} = \frac{4\left(a_0 - a_f\right)^6 + 6\left(a_0 - a_f\right)^4 \Delta a^2 + \left(a_0 - a_f\right)^2 \Delta a^4 + 4\Delta a^6}{5\left(a_0 - a_f\right)^2 \Delta a^3}$$

$$d_{0E}^{ai} = \frac{1}{\Delta a}$$

$$d_{1E}^{ai} = -\frac{\Delta a}{\left(a_0 - a_f\right)^2 - \Delta a^2} \tag{46}$$

$$d_{2E}^{ai} = -\frac{4\left(a_0 - a_f\right)^8 - 2\left(a_0 - a_f\right)^6 \Delta a^2 + 6\left(a_0 - a_f\right)^4 \Delta a^4 - 7\left(a_0 - a_f\right)^2 \Delta a^6 + 4\Delta a^8}{5\left(a_0 - a_f\right)^2 \Delta a^3 \left(\left(a_0 - a_f\right)^2 - \Delta a^2\right)^2}$$

$$d_{0F}^{et} = -\frac{\left(a_0 - a_f\right)^2 + \Delta a^2}{\left(a_0 - a_f\right)\Delta a}$$

$$d_{1F}^{et} = -\frac{\left(a_0 - a_f\right)^4 + 4\left(a_0 - a_f\right)^2 \Delta a^2 + 3\left(a_0 - a_f\right)\Delta a^3 + \Delta a^4}{3\left(a_0 - a_f\right)^2 \Delta a^2}$$

$$d_{2F}^{et} = \frac{22\left(a_0 - a_f\right)^6 + 10\left(a_0 - a_f\right)^5 \Delta a + 23\left(a_0 - a_f\right)^4 \Delta a^2}{30\left(a_0 - a_f\right)^3 \Delta a^3} \tag{47}$$

$$-\frac{20\left(a_0 - a_f\right)^3 \Delta a^3 + 7\left(a_0 - a_f\right)^2 \Delta a^4 + 20\left(a_0 - a_f\right)\Delta a^5 - 22\Delta a^6}{30\left(a_0 - a_f\right)^3 \Delta a^3}$$

$$d_{0E}^{et} = \frac{1}{\left(a_0 - a_f\right)\Delta a}$$

$$d_{1E}^{et} = \frac{\left(a_0 - a_f\right)^4 - 3\left(a_0 - a_f\right)\Delta a^3 - \Delta a^4}{3\left(a_0 - a_f\right)^2 \Delta a^2 \left(\left(a_0 - a_f\right)^2 - \Delta a^2\right)}$$

$$d_{2E}^{et} = -\frac{22\left(a_0 - a_f\right)^8 + 10\left(a_0 - a_f\right)^7 \Delta a - 21\left(a_0 - a_f\right)^6 \Delta a^2 - 10\left(a_0 - a_f\right)^5 \Delta a^3}{30\left(a_0 - a_f\right)^3 \Delta a^3 \left(\left(a_0 - a_f\right)^2 - \Delta a^2\right)^2} \tag{48}$$

$$-\frac{58\left(a_0 - a_f\right)^4 \Delta a^4 + 20\left(a_0 - a_f\right)^3 \Delta a^5 - 51\left(a_0 - a_f\right)^2 \Delta a^6 - 20\left(a_0 - a_f\right)\Delta a^7 + 22\Delta a^8}{30\left(a_0 - a_f\right)^3 \Delta a^3 \left(\left(a_0 - a_f\right)^2 - \Delta a^2\right)^2}$$

$$d_{0F}^{ei} = \frac{\left(a_0 - a_f\right)^4 + 10\left(a_0 - a_f\right)^2 \Delta a^2 + \Delta a^4}{3\left(a_0 - a_f\right)^2 \Delta a^2}$$

$$d_{1F}^{ei} = -\frac{\left(a_0 - a_f\right)^4 - 6\left(a_0 - a_f\right)^3 \Delta a - 5\left(a_0 - a_f\right)^2 \Delta a^2 - 6\left(a_0 - a_f\right)\Delta a^3 - 2\Delta a^4}{3\left(a_0 - a_f\right)^2 \Delta a^2}$$

$$d_{2F}^{ei} = -\frac{48\left(a_0 - a_f\right)^8 + 250\left(a_0 - a_f\right)^6 \Delta a^2 + 139\left(a_0 - a_f\right)^4 \Delta a^4}{105\left(a_0 - a_f\right)^4 \Delta a^4}$$

$$-\frac{210\left(a_0 - a_f\right)^3 \Delta a^5 - 145\left(a_0 - a_f\right)^2 \Delta a^6 - 48\Delta a^8}{105\left(a_0 - a_f\right)^4 \Delta a^4}$$

(49)

$$d_{0E}^{ei} = -\frac{\left(a_0 - a_f\right)^2 + \Delta a^2}{3\left(a_0 - a_f\right)^2 \Delta a^2}$$

$$d_{1E}^{ei} = \frac{\left(a_0 - a_f\right)^4 - 6\left(a_0 - a_f\right)^3 \Delta a + 3\left(a_0 - a_f\right)^2 \Delta a^2 + 6\left(a_0 - a_f\right)\Delta a^3 + 2\Delta a^4}{3\left(a_0 - a_f\right)^2 \Delta a^2 \left(\left(a_0 - a_f\right)^2 - \Delta a^2\right)}$$

$$d_{2E}^{ei} = \frac{48\left(a_0 - a_f\right)^{10} + 154\left(a_0 - a_f\right)^8 \Delta a^2 + 8\left(a_0 - a_f\right)^6 \Delta a^4 + 210\left(a_0 - a_f\right)^5 \Delta a^5}{105\left(a_0 - a_f\right)^4 \Delta a^4 \left(\left(a_0 - a_f\right)^2 - \Delta a^2\right)^2}$$

$$-\frac{97\left(a_0 - a_f\right)^4 \Delta a^6 + 210\left(a_0 - a_f\right)^3 \Delta a^7 - 49\left(a_0 - a_f\right)^2 \Delta a^8 - 48\Delta a^{10}}{105\left(a_0 - a_f\right)^4 \Delta a^4 \left(\left(a_0 - a_f\right)^2 - \Delta a^2\right)^2}$$

(50)

Eqs. (40) and (41) contain some elliptic integrals to be evaluated once per revolution:

$$elliF = EllipticF\left[\pi, \frac{4\left(a_0 - a_f\right)\Delta a}{\left(\left(a_0 - a_f\right) + \Delta a\right)^2}\right] - EllipticF\left[0, \frac{4\left(a_0 - a_f\right)\Delta a}{\left(\left(a_0 - a_f\right) + \Delta a\right)^2}\right]$$

(51)

where

$$EllipticF\left(\phi, \lambda\right) = \int_0^\phi \frac{1}{\sqrt{1 - \lambda \sin^2 \varphi}} \, d\varphi$$

(52)

is the first kind incomplete elliptic integral [13], and

$$elliE = EllipticE\left[\pi, \frac{4\left(a_0 - a_f\right)\Delta a}{\left(\left(a_0 - a_f\right) + \Delta a\right)^2}\right] - EllipticE\left[0, \frac{4\left(a_0 - a_f\right)\Delta a}{\left(\left(a_0 - a_f\right) + \Delta a\right)^2}\right]$$

(53)

where

$$EllipticE\left(\phi, \lambda\right) = \int_0^\phi \sqrt{1 - \lambda \sin^2 \varphi} \, d\varphi$$

(54)

is the second kind incomplete elliptic integral [13].

Numerical Results

To verify the accuracy of the semi-analytical solutions, a comparison is conducted between the semi-analytical solutions and the accurate integration of the full dynamics equations. The initial and stopping conditions for the test case of the orbit raising mission are listed in Table 3, while the spacecraft characteristics and the parameters for the de-orbit mission have been listed in Table 1 and Table 2 respectively.

Table 3 Parameters for the orbit raising mission

| Initial condition				Stopping condition	
a_0 (km)	e_0	ω_0 (deg)	E_0 (deg)	a_f (km)	e_f
$500 + R_E$	10^{-3}	0	0	$1200 + R_E$	$\leq 10^{-4}$

Figure 5 to Figure 10 present the time histories of the orbital parameters by the accurate integration and the semi-analytical integration for both missions. From Figure 5, Figure 6, Figure 8 and Figure 9, it can be seen the good accuracy of the semi-analytical solutions for the semi-major axis and eccentricity. In Figure 7, the semi-analytical solution for the argument of perigee during the orbit raising mission shows a good accuracy up to $e = 10^{-4}$ until the eccentricity is too small that the accurate integration breaks down, being written in Keplerian elements. While in Figure 10, the semi-analytical solution for the argument of perigee during the de-orbit mission has relatively large errors, which might be due to the singularity in the derivatives for the argument of perigee and the eccentric anomaly (Eqs. (3) and (4)) because the initial eccentricity of the de-orbit mission is too small (10^{-4}). This could be furtherly solved by using non-singular orbital elements.
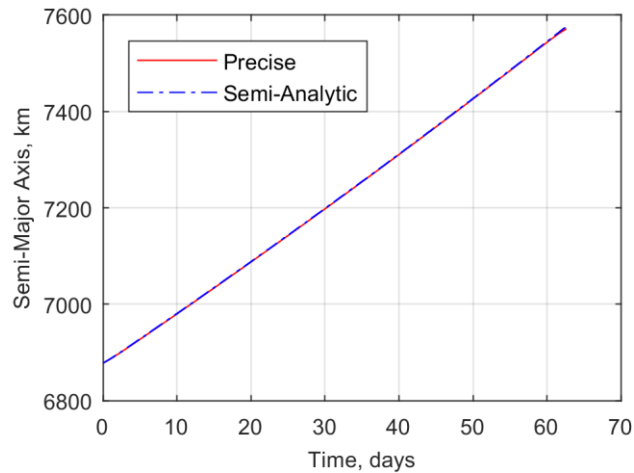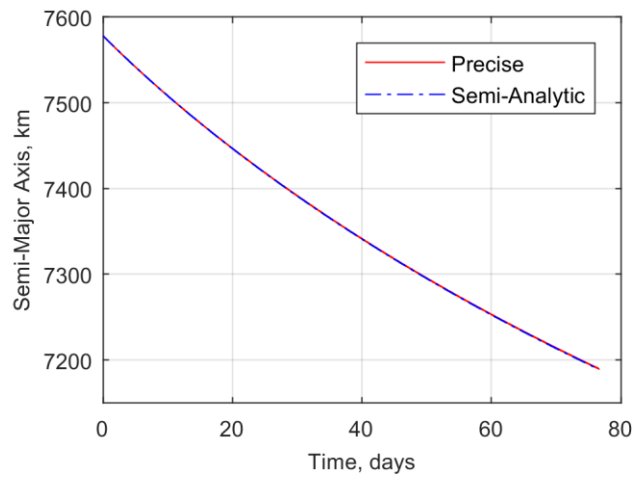

Figure 5 Time history of the semi-major axis for the orbit raising mission.
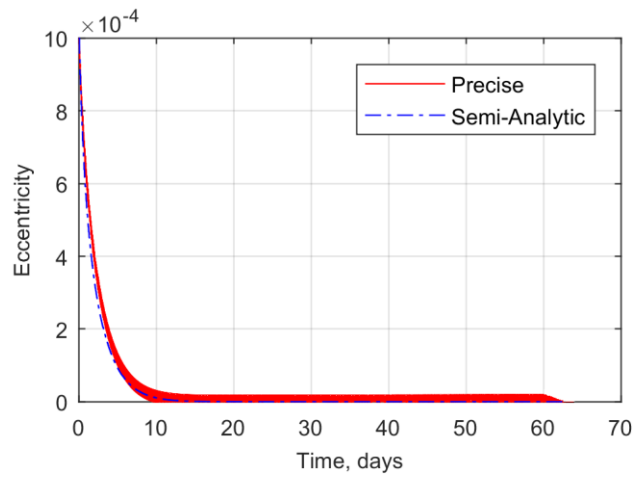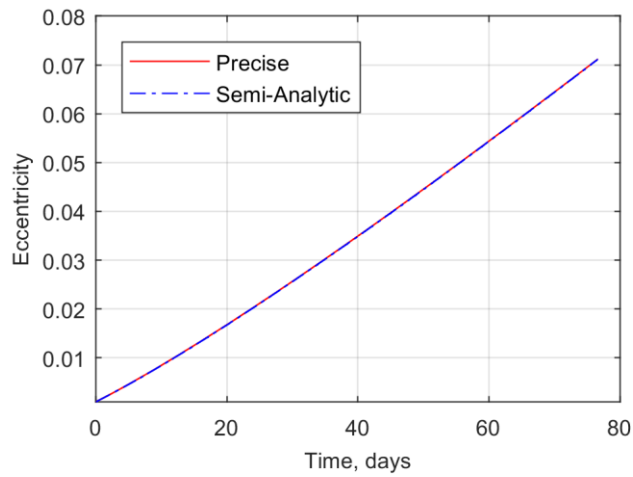
Figure 6 Time history of the eccentricity for the orbit raising mission.
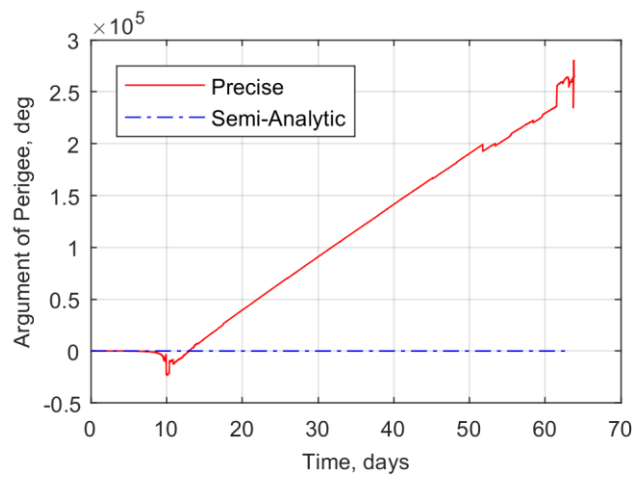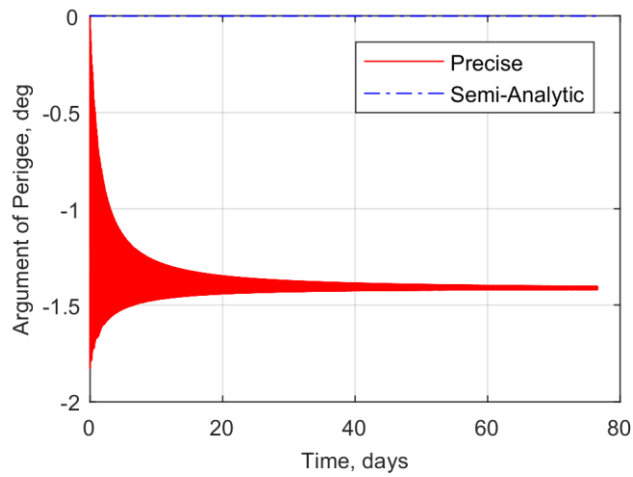

Figure 7 Time history of the argument of perigee for the orbit raising mission.

Figure 8 Time history of semi-major axis for de-orbit mission.

Figure 9 Time history of the eccentricity for the de-orbit mission.

Figure 10 Time history of the argument of the perigee for the de-orbit mission.

Table 4 presents the results obtained by the semi-analytical technique and the precise integration. The results show good agreement between the two methods.

Table 4 Results by the semi-analytic technique and the precise integration

Mission	Semi-analytical technique			Precise integration		
	a_f (km)	e_f	t_f (days)	a_f (km)	e_f	t_f (days)
Orbit raising	7578.2	4×10^{-7}	62.85	7578.5	4×10^{-7}	62.86
De-orbiting	7189.0	0.0711	76.63	7189.4	0.0712	76.63

## ORBIT TRANSFER FOR MULTIPLE SATELLITES

The collision problem will arise when transferring multiple satellites. The mission objective is now not only the minimization of total transfer time, but also the maximization of the inter-satellite miss distance. In this study, the miss distance is the minimum distance between any pair

of satellites in the constellation during transfer. The miss distance can be derived by evaluating the relative distances for all pairs of satellites at every time step. This computation process needs the transfer trajectories of all satellites, which can be easily obtained by the semi-analytical solutions.

Miss Distance Analysis

Figure 11 and Figure 12 presents the miss distance as a function of the time difference at which the transfer among the satellites is started in terms of different argument of perigee difference for the orbit raising and de-orbiting mission respectively. In these graphs, $\Delta\omega = 1 \times 2\pi/8$ is the argument of perigee difference between a satellite and the first successive satellite; $\Delta\omega = 2 \times 2\pi/8$ is the argument of perigee difference between a satellite and the second successive satellite, etc. For the test case of this paper, the constellation consists of 8 evenly spaced satellites and the relative distance is evaluated at time intervals of 100 s. The mission conditions are same as the previous sections.

a) Time difference $\leq 5 \times 10^4$ s b) Time difference $\geq 4 \times 10^4$ s
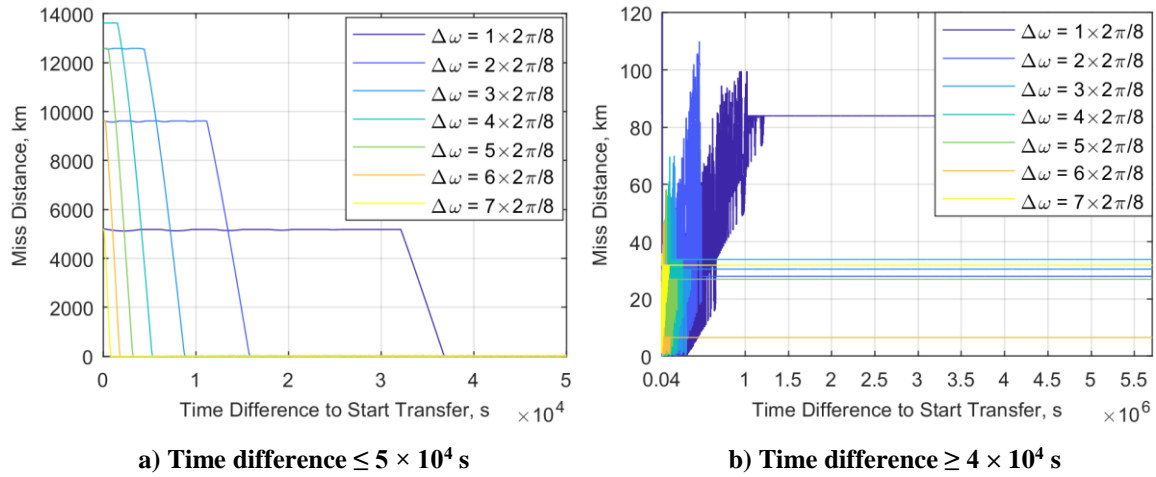
Figure 11 Miss distance vs time difference to start the transfer for the orbit raising mission.

a) Time difference $\leq 1 \times 10^4$ s b) Time difference $\geq 1 \times 10^4$ s
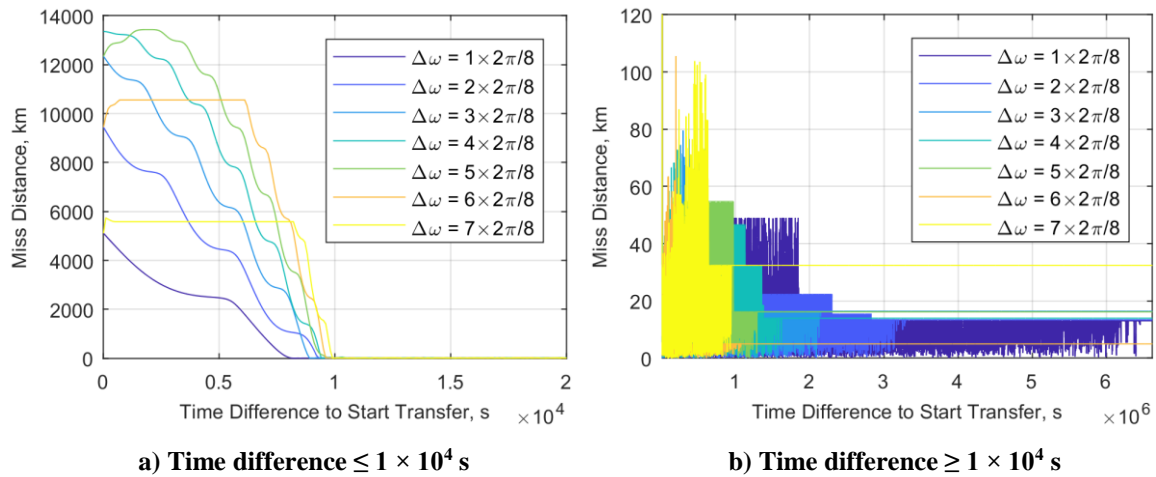
Figure 12 Miss distance vs time difference to start the transfer for the de-orbiting mission.

It can be seen from the above figures that for both missions, the miss distances for all pairs of

111

satellites maintain relatively large if the starting time difference is within the first few revolutions, but then decline rapidly to dozens or even several kilometers as the starting time difference increases.

The reason behind this is the resonance of longitudes. Here, the notation longitude is the sum of argument of perigee and true anomaly. The relative distance between a pair of satellites not only depends on the radii difference but also the longitude difference. The resonance of the longitude is the longitude difference being equal to integral multiple of 2π rad, at which instant the satellites pass by each other and the relative distance is small. In this case, the miss distance will be accordingly small.

Specifically in this paper, the resonance of longitude is equivalent to the resonance of the true anomaly because the argument of perigee solved by the semi-analytic technique does not change with time. The derivative of the true anomaly given by the Gauss' equations[7] is

$$\frac{\mathrm{d}\theta}{\mathrm{d}t} = \frac{h^2}{r} + \frac{1}{eh}\left[p\cos\theta T_r - (p+r)\sin\theta T_\theta \right] \tag{55}$$

Similar with $\mathrm{d}E/\mathrm{d}t$, $\mathrm{d}\theta/\mathrm{d}t$ can be approximated as

$$\frac{\mathrm{d}\theta}{\mathrm{d}t} \approx \frac{h}{r^2} = \sqrt{\frac{\mu(1-e^2)}{a^3}} \frac{1}{(1-e\cos E)^2} \tag{56}$$

It can be seen from Eq. (56) that the magnitude of $\mathrm{d}\theta/\mathrm{d}t$ is dictated by the semi-major axis and the eccentricity. For two trajectories, the small difference of semi-major axis and eccentricity leads to small difference of the magnitude of $\mathrm{d}\theta/\mathrm{d}t$ and consequently in true anomaly.

Take the argument difference of $1\times 2\pi/8$ for the de-orbit mission as an example. Figure 13 to Figure 15 present the time histories of the semi-major axis, eccentricity and longitude difference as well as $\cos\Delta(\omega + \theta)$ and the relative distance for the starting time difference of 5×10^3 s and 1.4×10^6 s.

a) Time difference = 5×10^3 s   b) Time difference = 1.4×10^6 s
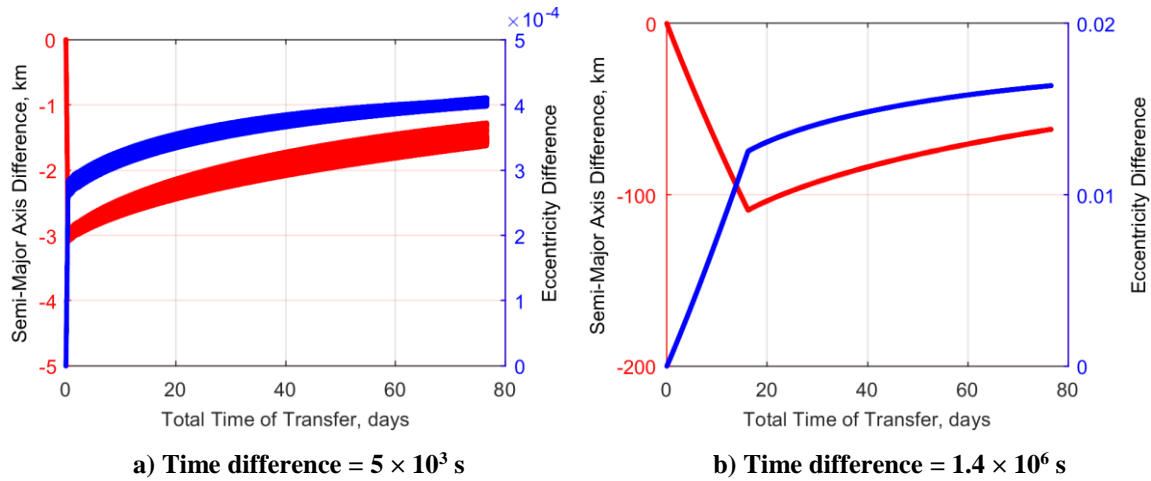
Figure 13 Time histories of the semi-major axis and the eccentricity (de-orbit, $\Delta\omega = 1\times 2\pi/8$).

a) Time difference = 5×10^3 s   b) Time difference = 1.4×10^6 s
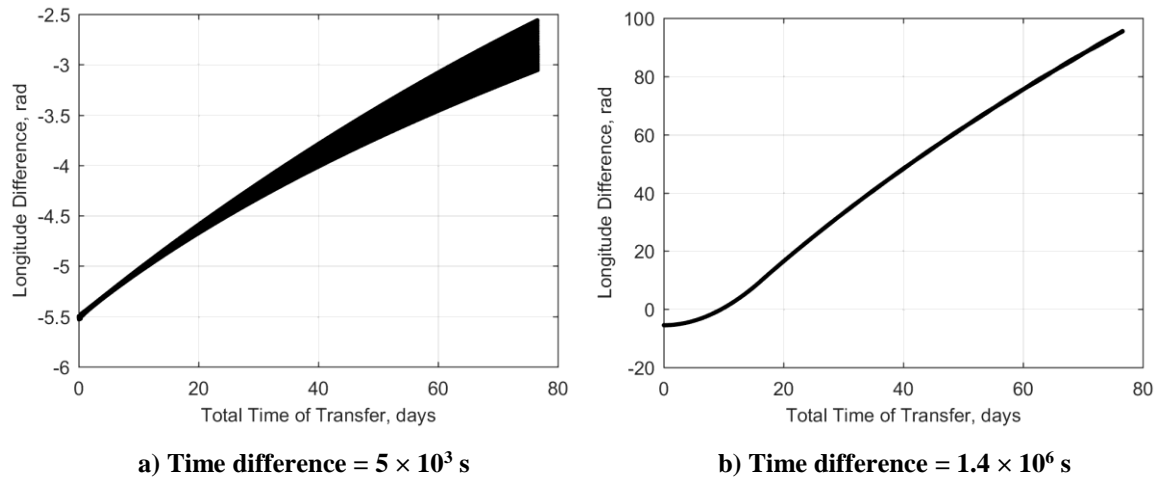
Figure 14 Time histories of the true anomaly (de-orbit, $\Delta\omega = 1 \times 2\pi/8$).

a) Time difference = 5×10^3 s   b) Time difference = 1.4×10^6 s
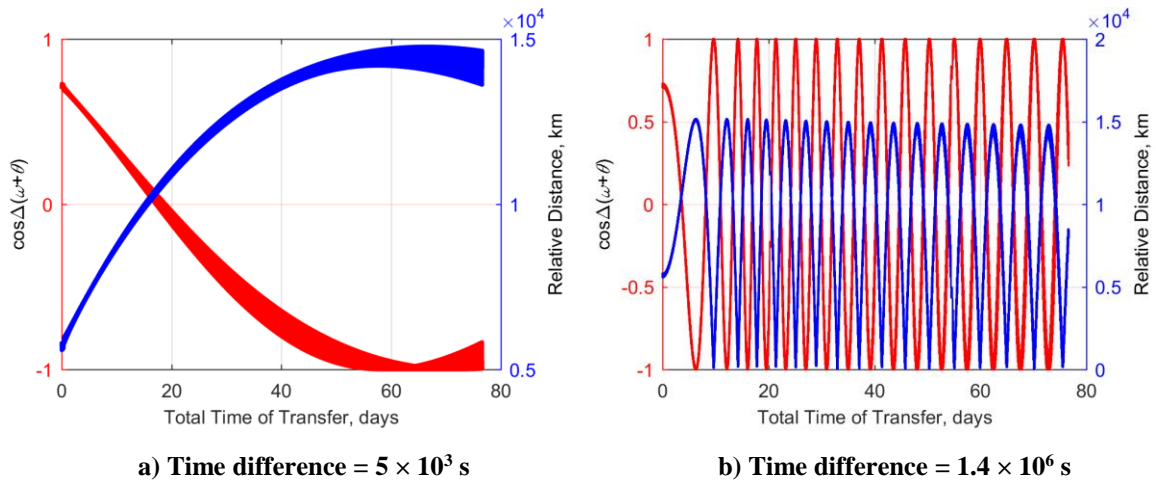
Figure 15 Time histories of cos$\Delta(\omega + \theta)$ and relative distance (de-orbit, $\Delta\omega = 1 \times 2\pi/8$).

For small starting time difference, the semi-major axis difference and the eccentricity difference are both small, as shown in Figure 13 a). Therefore, the longitude difference increases slowly with time and will not be able to reach zero, as shown in Figure 14 a). This means that no resonance happens so that the miss distance is relatively large, as shown in Figure 15 a). While for large starting time difference, the semi-major axis difference and the eccentricity difference are both large, as shown in Figure 13 b). Therefore, the longitude difference increases fast with time, as shown in Figure 14 b). So the resonance happens many times and the miss distance is small, as shown in Figure 15 b).

Transfer Strategy

According to Figure 11 and Figure 12, obviously for both missions, the best orbit transfer strategy is to start the transfer for all satellites at the same time such that the total time of transfer is minimum while the miss distance is maximum.

For no doubts in orbit raising mission, it is favorable that the satellites start to raise orbits at the same time so that the constellation can provide services to the Earth as soon as possible. But

for de-orbit mission, there might exist some limits on the descending starting time. To maximize profits in practical applications, it might be desirable to retain residual performances during de-orbiting. That is to say, the satellites start to de-orbit at different times such that some of the satellites keep providing services to the Earth while the others are de-orbiting.

Noticing from Figure 12, the miss distance between satellites in opposite positions, i.e., $\Delta\omega = 4\times 2\pi/8$, is maximum if the two satellites start to de-orbit at the same time. Moreover, from geometric point of view, it is always preferable to hold the constellation structure symmetric so as to maximize the residual performances (e.g., coverage and robustness). For these two reasons, four types of de-orbit strategy are proposed for the test case of 8 satellites constellation. As shown in Figure 16, in strategy 1, the satellites start to de-orbit at the same time in groups of four, while in strategy $2 - 4$, the satellites start to de-orbit in groups of two. In these graphs, t_0, t_1, t_2 and t_3 represent the starting time to de-orbit.
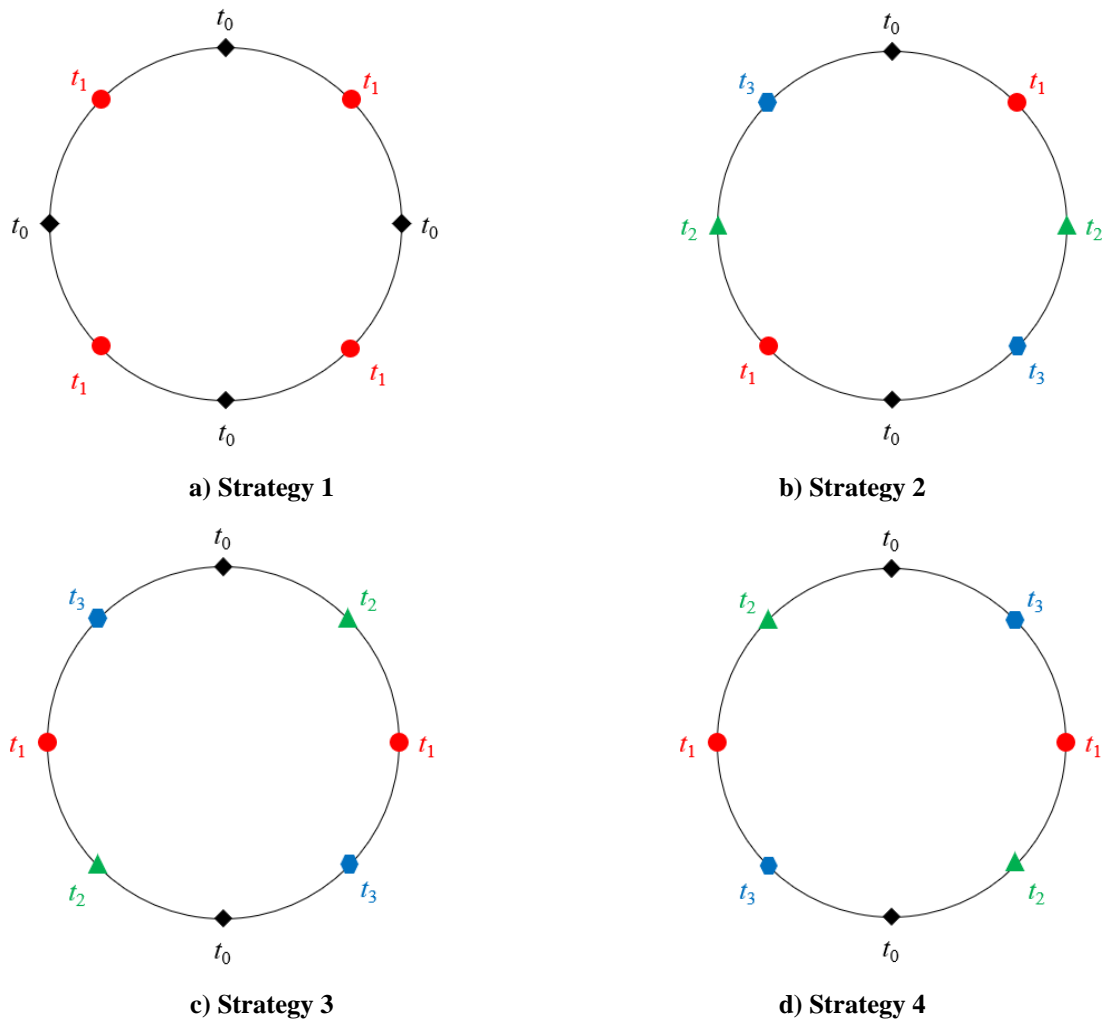
a) Strategy 1

b) Strategy 2

c) Strategy 3

d) Strategy 4

Figure 16 De-orbiting strategies.

Multi-Objective Optimization

The cost functions of the multi-objective optimization problem are given by

114

$$J_1 = \min t_{total} \tag{57}$$

$$J_2 = -\min d_{miss} \tag{58}$$

where, t_{total} is the total time of transfer and d_{miss} is the miss distance.

The design variable is the starting time, i.e., t_1 for Strategy 1, t_1, t_2 and t_3 for Strategy 2 – 4. Assume that the constellation has to be de-orbited within 3.5 months. According to the numerical results by previous sections, the de-orbit time for a single satellite is about 2.5 months. Thus, all satellites have to start de-orbit within 1 month. The lower and upper bounds for starting time are listed in Table 5. A multi-objective global optimizer is used to search for the Pareto front solutions through a multi-agent-based search approach hybridized with a domain decomposition technique developed by Vasile[14].

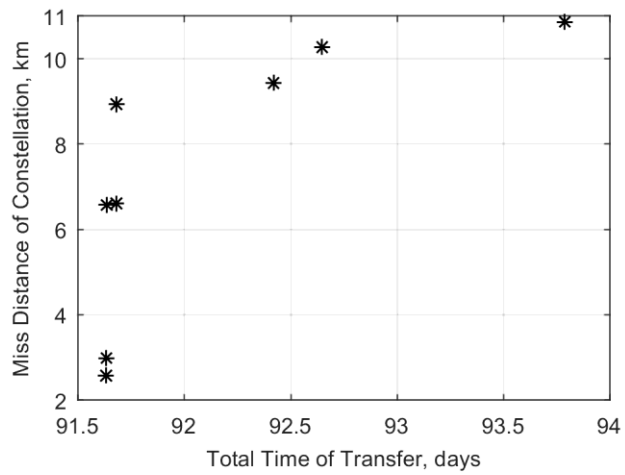**Table 5 Lower and upper bounds for the starting time**

Strategy	t_0 (days)	Lower bound			Upper bound (days)		
		t_1 (days)	t_2 (days)	t_3 (days)	t_1 (days)	t_2 (days)	t_3 (days)
1	0	15			30		
2 – 4	0	7.5	15	22.5	30	30	30

Figure 17 presents the optimization results for Strategy 1.
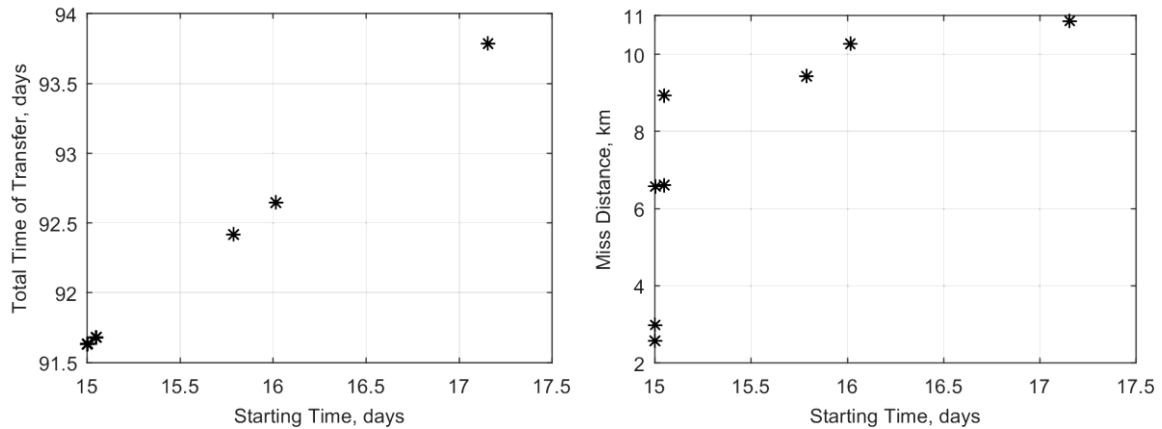
a) **Total time of transfer vs starting time**   b) **Miss distance vs starting time**

c) Total Time of transfer vs starting time

Figure 17 Optimization results for strategy 1.

Figure 18 to Figure 20 present the optimization results for Strategy 2 to 4. Although only one set of Pareto front is found, there is a series of starting time resulting in the same transfer time and miss distance.
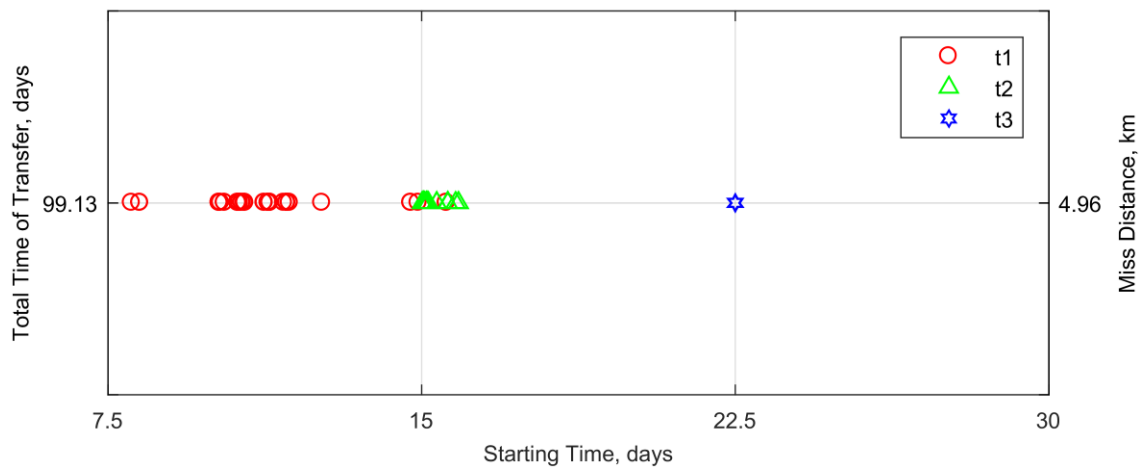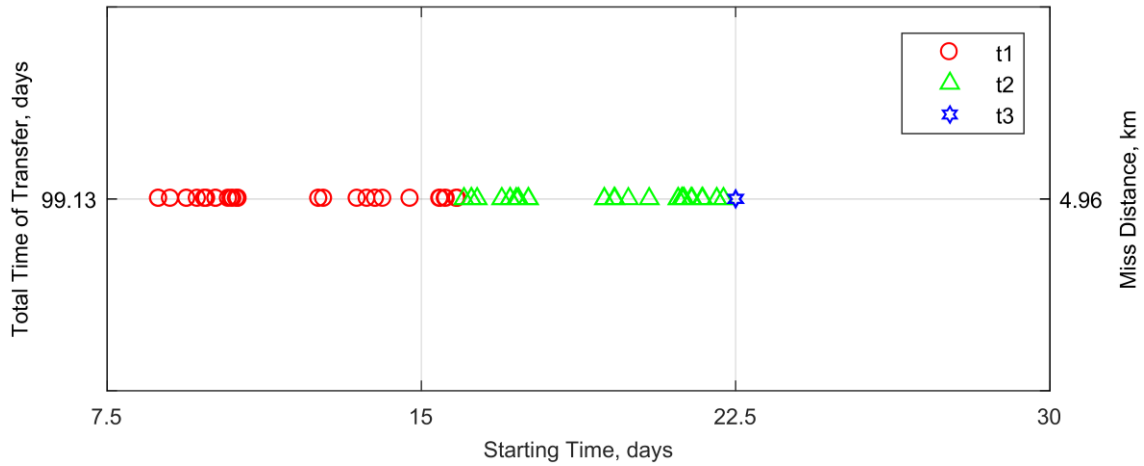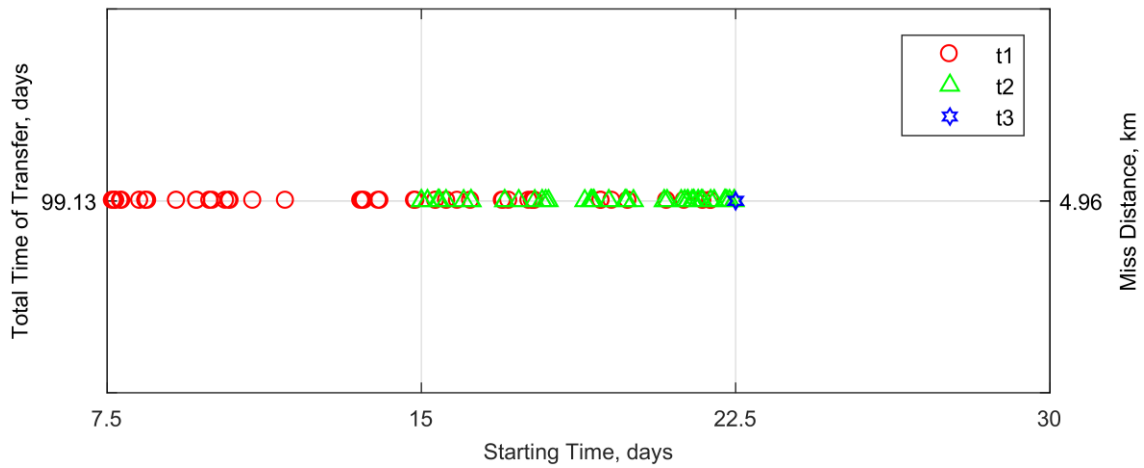

Figure 18 Optimization results for strategy 2.

Figure 19 Optimization results for strategy 3.

Figure 20 Optimization results for strategy 4.

The detailed optimization results for each strategy are listed in Table 6 to Table 9 in Appendix: Optimization Results.

Comparing the optimization results of these four strategies, Strategy 1 has shorter transfer time and larger miss distance than Strategy 2 – 4, but more residual performance is retained by Strategy 2 – 4. Therefore, one conclusion can be drawn: there is a trade-off between residual performance, total time of transfer and miss distance.

CONCLUSION

This paper dealt with the planar transfer problems (orbit raising and de-orbiting) for LEO co-planar satellites constellation with low-thrust propulsion. Aiming to solve the collision problem arising at the presence of multiple satellites, the objectives of this paper are to minimize the total time of transfer and to maximize the miss distance. The orbit transfer problem has been conducted via two layers: the first layer is the trajectory design for a single satellite; the second layer is the transfer strategy design and the multi-objective optimization for multiple satellites.

For the first layer, the blended error-correction (BEC) steering law has been firstly presented.

The BEC steering law is the blend of tangential thrust and inertial thrust, both of them being time efficient and in simple fashion. The coefficients of tangential thrust and inertial thrust are respectively set to be proportional to the instantaneous errors of semi-major axis and eccentricity with respect to the target values, and are properly normalized. The numerical comparison with the optimal steering law for the test case of de-orbit shows that the BEC steering law is feasible and near time-optimal. Based on the BEC steering law, two sets of semi-analytical solutions of the variations of orbital parameters over one revolution for orbit raising and de-orbit have been obtained by using the semi-analytical technique so as to reduce the computation load. Before integrating, the denominator of coefficients is expanded in powers of eccentricity up to $O(e^2)$. The numerical comparison with the precise integration shows a good accuracy of the semi-analytical solutions.

For the second layer, a detailed analysis has been firstly done for the miss distance, revealing the influence of longitude resonance on the miss distance. The analysis shows that the best transfer strategy is to start to transfer all satellites at the same time. Considering the limits on the transfer starting time for de-orbit mission, four transfer strategies for a test case of 8 satellites constellations have been proposed. For each strategy, a multi-objective optimization has been carried out. The design variable is the transfer starting time of each satellite. The optimization results show the trade-off between residual performance, total time of transfer and miss distance.

As a preliminary study, the Earth's oblateness and the eclipses are not considered in this paper. Further research will include theses effects and extend the planar transfer to non-planar transfer.

ACKNOWLEDGMENTS

APPENDIX: OPTIMIZATION RESULTS

Table 6 Optimization Results for Strategy 1.

t_1 (days)	Total time of transfer (days)	Miss distance (km)
15	91.6319	2.5757
15.0012	91.6331	2.9834
15.0023	91.6343	6.5720
15.0475	91.6794	6.6081
15.0486	91.6806	8.9317
15.7870	92.4190	9.4330
16.0150	92.6470	10.2728
17.1551	93.7870	10.8619

Table 7 Optimization results for strategy 2.

(Total time of transfer = 99.13 days, Miss distance = 4.96 km)

t_1 (days)	t_2 (days)	t_3 (days)

8.07	15.16	22.5
8.27	15.36	22.5
10.17	15.01	22.5
10.20	15.01	22.5
10.29	15.02	22.5
10.61	15.06	22.5
10.65	15.05	22.5
10.71	15.02	22.5
10.76	15.81	22.5
10.78	15.05	22.5
11.24	15.11	22.5
11.34	15.04	22.5
11.38	15.13	22.5
11.70	15.07	22.5
11.78	15.05	22.5
11.84	15.88	22.5
12.62	15.12	22.5
14.75	15.62	22.5
14.93	15.62	22.5
15.59	15.05	22.5

Table 8 Optimization results for strategy 3.

(Total time of transfer = 99.13 days, Miss distance = 4.96 km)

t_1 (days)	t_2 (days)	t_3 (days)
8.74	22.05	22.5
9.02	21.23	22.5
9.41	19.37	22.5
9.67	16.02	22.5
9.84	19.61	22.5
9.89	19.62	22.5
10.11	17.55	22.5
10.41	22.21	22.5
10.47	22.21	22.5
10.51	17.31	22.5
10.60	21.70	22.5

10.64	21.72	22.5
10.64	21.72	22.5
12.55	20.44	22.5
12.68	21.46	22.5
13.48	21.26	22.5
13.71	21.27	22.5
13.91	19.94	22.5
13.92	21.22	22.5
14.09	21.12	22.5
14.74	21.13	22.5
15.45	17.12	22.5
15.47	16.92	22.5
15.58	17.12	22.5
15.61	17.27	22.5
15.85	16.33	22.5
15.87	16.19	22.5

Table 9 Optimization results for strategy 4.

(Total Time of transfer = 99.13 days, Miss distance = 4.96 km)

t_1 (days)	t_2 (days)	t_3 (days)
7.64	21.46	22.5
7.67	20.06	22.5
7.71	15	22.5
7.71	21.28	22.5
7.72	19.90	22.5
7.72	21.36	22.5
7.83	19.07	22.5
7.86	21.99	22.5
8.29	19.11	22.5
8.29	19.12	22.5
8.43	21.50	22.5
8.44	21.50	22.5
8.48	21.36	22.5
9.17	21.90	22.5
9.65	21.61	22.5

9.97	15	22.5
9.97	20.80	22.5
10.03	21.68	22.5
10.34	16.01	22.5
10.41	15	22.5
10.44	15	22.5
10.45	18.90	22.5
10.98	22.29	22.5
11.76	21.71	22.5
13.56	19.86	22.5
13.61	15.42	22.5
13.62	15.43	22.5
13.65	15.41	22.5
13.99	15	22.5
14.01	15	22.5
14.02	22.47	22.5
14.85	15.15	22.5
14.85	15.14	22.5
14.88	19.86	22.5
15.35	19.48	22.5
15.62	19.04	22.5
15.87	15.39	22.5
16.19	15	22.5
16.94	15	22.5
16.97	17.97	22.5
17.09	17.70	22.5
17.58	21.20	22.5
17.66	17.88	22.5
17.70	22.24	22.5
17.71	17.33	22.5
19.30	16.99	22.5
19.56	22.26	22.5
19.94	15.59	22.5
20.87	20.87	22.5

21.26	20.79	22.5
21.73	22.35	22.5
21.91	16.19	22.5
21.92	16.18	22.5
21.92	16.19	22.5
21.92	18.03	22.5

REFERENCES

[1] https://en.wikipedia.org/wiki/OneWeb_satellite_constellation

[2] B.B. Virgili, J.C. Dolado, H.G. Lewis, J. Radtke, H. Krag, B. Revelin, C. Cazaux, C. Colombo, R. Crowther and M. Metz. "Risk to Space Sustainability from Large Constellations of Satellites." *Acta Astronautica*. Vol. 126, 2016, pp. 154-162.

[3] J. Radtke, K. Christopher and E. Stoll. "Interactions of the space debris environment with mega constellations—Using the example of the OneWeb constellation." *Acta Astronautica*. Vol. 131, 2017, pp. 55-68.

[4] A. Ruggiero, P. Pergola, S. Marcuccio and M. Andrenucci. "Low-Thrust Maneuvers for the Efficient Correction of Orbital Elements." *32nd International Electric Propulsion Conference*, 2011, pp. 11-15.

[5] Y. Gao. "Near-Optimal Very Low-Thrust Earth-Orbit Transfers and Guidance Schemes." *Journal of Guidance, Control, and Dynamics*. Vol. 30, No. 2, 2007, pp. 529-539.

[6] C.A. Kluever and S.R. Oleson. "Direct Approach for Computing Near-Optimal Low-Thrust Earth-Orbit Transfers." *Journal of Spacecraft and Rockets*. Vol. 35, No. 4, 1998, pp. 509-515.

[7] R.H. Battin. An Introduction to the Mathematics and Methods of Astrodynamics. AIAA, 1999. pp. 488-489.

[8] J. Yang and J. Fan. Orbit Dynamics and Control of Spacecraft. Beijing: China Astronautic Publishing House, 1995, pp. 62-63.

[9] Y. Gao and C.A. Kluever. "Analytic Orbital Averaging Technique for Computing Tangential-Thrust Trajectories." *Journal of Guidance, Control, and Dynamics*. Vol. 28, No. 6, 2005, pp. 1320-1323.

[10] A. Spitzer. "Near Optimal Transfer Orbit Trajectory Using Electric Propulsion," *Advances in the Astronautical Sciences*, American Astronautical Society, San Diego, CA, Vol. 89, 1995, pp. 1013-1044.

[11] A. Gaudel, C. Hourtolle, J.F. Goester, N. Fuentes and M. Ottaviani. "De-Orbit Strategies with Low-Thrust Propulsion." *Space Safety is No Accident.* Springer, Cham, 2015. pp. 59-68.

[12] J.A. Kechichian. "Orbit Raising with Low-Thrust Tangential Acceleration in Presence of Earth Shadow." *Journal of Spacecraft and Rockets*. Vol. 35, No. 4, 1998, pp. 516-525.

[13] R.H. Battin. An Introduction to the Mathematics and Methods of Astrodynamics. AIAA, 1999. pp. 68-78.

[14] M. Vasile. "Robust Mission Design Through Evidence Theory and Multiagent Collaborative Search." *Annals of the New York Academy of Sciences*, Vol. 1065, No. 1, pp. 152–173.